Supernovae as stellar objects

W. Hillebrandt, M. Reinecke, J.C. Niemeyer
Max-Planck-Institut für Astrophysik, Garching, Germany

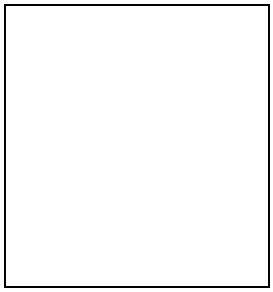

Type Ia supernovae (SN Ia) are generally believed to be the result of the thermonuclear disruption of Chandrasekhar-mass carbon-oxygen white dwarfs, mainly because such thermonuclear explosions can account for the right amount of ^{56}Ni, which is needed to explain the light curves and the late-time spectra, and the abundances of intermediate-mass nuclei which dominate the spectra near maximum light. Because of their enormous brightness and apparent homogeneity SN Ia have become an important tool to measure cosmological parameters. In this article the present understanding of the physics of thermonuclear explosions is reviewed. In particular, we focus our attention on subsonic ("deflagration") fronts, i.e. we investigate fronts propagating by heat diffusion and convection rather than by compression. Models based upon this mode of nuclear burning have been applied very successfully to the SN Ia problem, and are able to reproduce many of their observed features remarkably well. However, the models also indicate that SN Ia may differ considerably from each other, which is of importance if they are to be used as standard candles.

1 Introduction

Type Ia supernovae, i.e. stellar explosions which do not have hydrogen in their spectra, but intermediate-mass elements, such as silicon, calcium, cobalt, and iron, have recently received considerable attention because it appears that they can be used as "standard candles" to measure cosmic distances out to billions of light years away from us. Moreover, observations of type Ia supernovae seem to indicate that we are living in a universe that started to accelerate its expansion when it was about half its present age. These conclusions rest primarily on phenomenological models which, however, lack proper theoretical understanding, mainly because the explosion process, initiated by thermonuclear fusion of carbon and oxygen into heavier elements, is difficult to simulate even on supercomputers, for reasons we shall discuss in this article.

The most popular progenitor model for the average type Ia supernovae is a massive white dwarf, consisting of carbon and oxygen, which approaches the Chandrasekhar mass, $M_{\rm Ch} \approx$

$1.39 M_\odot$, by a yet unknown mechanism, presumably accretion from a companion star, and is disrupted by a thermonuclear explosion[44]. Arguments in favor of this hypothesis include the ability of the models to fit the observed spectra and light curves rather well.

However, not only is the evolution of massive white dwarfs to explosion very uncertain, leaving room for some diversity in the initial conditions (such as the temperature profile at ignition), but also the physics of thermonuclear burning in degenerate matter is complex and not well understood. The generally accepted scenario is that explosive carbon burning is ignited either at the center of the star or off-center in a couple of ignition spots, depending on the details of the previous evolution. After ignition, the flame is thought to propagate through the star as a subsonic deflagration wave which may or may not change into a detonation at low densities (around $10^7 \mathrm{g/cm}^3$). Numerical models with parameterized velocity of the burning front have been very successful, the prototype being the W7 model of Nomoto et al.[28]. However, these models do not solve the problem because attempts to determine the effective flame velocity from direct numerical simulations failed and gave velocities far too low for successful explosions[19,13,1]. This has led to some speculations about ways to change the deflagration into a supersonic detonation[9,10]. Some of these aspects of supernova models will be discussed in the following sections.

2 Nuclear burning in degenerate C+O matter

Owing to the strong temperature dependence of the nuclear reaction rates nuclear burning during the explosion is confined to microscopically thin layers that propagate either conductively as subsonic deflagrations ("flames") or by shock compression as supersonic detonations[4,16]. Both modes are hydrodynamically unstable to spatial perturbations as can be shown by linear perturbation analysis. In the nonlinear regime, the burning fronts are either stabilized by forming a cellular structure or become fully turbulent – either way, the total burning rate increases as a result of flame surface growth[18,42,46]. Neither flames nor detonations can be resolved in explosion simulations on stellar scales and therefore have to be represented by numerical models.

When the fuel exceeds a critical temperature T_c where burning proceeds nearly instantaneously compared with the fluid motions, a thin reaction zone forms at the interface between burned and unburned material. It propagates into the surrounding fuel by one of two mechanisms allowed by the Rankine-Hugoniot jump conditions: a deflagration ("flame") or a detonation.

If the overpressure created by the heat of the burning products is sufficiently high, a hydrodynamical shock wave forms that ignites the fuel by compressional heating. Such a self-sustaining combustion front that propagates by shock-heating is called a detonation. If, on the other hand, the initial overpressure is too weak, the temperature gradient at the fuel-ashes interface steepens until an equilibrium between heat diffusion and energy generation is reached. The resulting combustion front consists of a diffusion zone that heats up the fuel to T_c, followed by a thin reaction layer where the fuel is consumed and energy is generated. It is called a deflagration or simply a flame and moves subsonically with respect to the unburned material [16]. Flames, unlike detonations, may therefore be strongly affected by turbulent velocity fluctuations of the fuel. Only if the unburned material is at rest, a unique laminar flame speed S_l can be found which depends on the detailed interaction of burning and diffusion within the flame region[46]. It can be estimated by assuming that in order for burning and diffusion to be in equilibrium, the respective time scales, $\tau_\mathrm{b} \sim \epsilon/\dot{w}$ and $\tau_\mathrm{d} \sim \delta^2/\kappa$, where δ is the flame thickness and κ is the thermal diffusivity, must be similar[16]: $\tau_\mathrm{b} \sim \tau_\mathrm{d}$. Defining $S_\mathrm{l} = \delta/\tau_\mathrm{b}$, one finds $S_\mathrm{l} \sim (\kappa \dot{w}/\epsilon)^{1/2}$, where $\dot{w}$ should be evaluated at $T \approx T_\mathrm{c}$ ([41]). This is only a crude estimate due to the strong T-dependence of $\dot{w}$. Numerical solutions of the full equations of hydrodynam-

ics including nuclear energy generation and heat diffusion are needed to obtain more accurate values for $S_{\rm l}$ as a function of ρ and fuel composition. Laminar thermonuclear carbon and oxygen flames at high to intermediate densities were investigated[2,8,43], and, using a variety of different techniques and nuclear networks, by Timmes & Woosley[41]. For the purpose of SN Ia explosion modeling, one needs to know the laminar flame speed $S_{\rm l} \approx 10^7 \ldots 10^4$ cm s^{-1} for $\rho \approx 10^9 \ldots 10^7$ g cm^{-3}, the flame thickness $\delta = 10^{-4} \ldots 1$ cm (defined here as the width of the thermal pre-heating layer ahead of the much thinner reaction front), and the density contrast between burned and unburned material $\mu = \Delta\rho/\rho = 0.2 \ldots 0.5$ (all values quoted here assume a composition of $X_{\rm C} = X_{\rm O} = 0.5$[41]). The thermal expansion parameter μ reflects the partial lifting of electron degeneracy in the burning products, and is much lower than the typical value found in chemical, ideal gas systems[42].

3 Hydrodynamic instabilities and turbulence

The best studied and probably most important hydrodynamical effect for modeling SN Ia explosions is the Rayleigh-Taylor (RT) instability resulting from the buoyancy of hot, burned fluid with respect to the dense, unburned material[21,22,19,12,13,24], and after more than five decades of experimental and numerical work, the basic phenomenology of nonlinear RT mixing is fairly well understood[6,17,38,34,45]: Subject to the RT instability, small surface perturbations grow until they form bubbles (or "mushrooms") that begin to float upward while spikes of dense fluid fall down. In the nonlinear regime bubbles of various sizes interact and create a foamy RT mixing layer whose vertical extent $h_{\rm RT}$ grows with time t according to a self-similar growth law, $h_{\rm RT} = \alpha g(\mu/2)t^2$, where α is a dimensionless constant ($\alpha \approx 0.05$) and g is the background gravitational acceleration.

Secondary instabilities related to the velocity shear along the bubble surfaces[25] quickly lead to the production of turbulent velocity fluctuations that cascade from the size of the largest bubbles ($\approx 10^7$ cm) down to the microscopic Kolmogorov scale, $l_{\rm k} \approx 10^{-4}$ cm where they are dissipated[24,13]. Since no computer is capable of resolving this range of scales, one has to resort to statistical or scaling approximations of those length scales that are not properly resolved. The most prominent scaling relation in turbulence research is Kolmogorov's law for the cascade of velocity fluctuations, stating that in the case of isotropy and statistical stationarity, the mean velocity v of turbulent eddies with size l scales as $v \sim l^{1/3}$ ([15]). Given the velocity of large eddies, e.g. from computer simulations, one can use this relation to extrapolate the eddy velocity distribution down to smaller scales under the assumption of isotropic, fully developed turbulence[24]. Knowledge of the eddy velocity as a function of length scale is important to classify the burning regime of the turbulent combustion front[27,26,14]. The ratio of the laminar flame speed and the turbulent velocity on the scale of the flame thickness, $K = S_{\rm l}/v(\delta)$, plays an important role: if $K \gg 1$, the laminar flame structure is nearly unaffected by turbulent fluctuations. Turbulence does, however, wrinkle and deform the flame on scales l where $S_{\rm l} \ll v(l)$, i.e. above the *Gibson scale* $l_{\rm g}$ defined by[31] $S_{\rm l} = v(l_{\rm g})$. These wrinkles increase the flame surface area and therefore the total energy generation rate of the turbulent front[5]. In other words, the turbulent flame speed, $S_{\rm t}$, defined as the mean overall propagation velocity of the turbulent flame front, becomes larger than the laminar speed $S_{\rm l}$. If the turbulence is sufficiently strong, $v(L) \gg S_{\rm l}$, the turbulent flame speed becomes independent of the laminar speed, and therefore of the microphysics of burning and diffusion, and scales only with the velocity of the largest turbulent eddy[5,3]:

$$S_{\rm t} \sim v(L) \ . \tag{1}$$

Because of the unperturbed laminar flame properties on very small scales, and the wrinkling of the flame on large scales, the burning regime where $K \gg 1$ is called the corrugated flamelet

regime[33,3].

As the density of the white dwarf material declines and the laminar flamelets become slower and thicker, it is plausible that at some point turbulence significantly alters the thermal flame structure[14,27]. This marks the end of the flamelet regime and the beginning of the distributed burning, or distributed reaction zone, regime[33]. So far, modeling the distributed burning regime in exploding white dwarfs has not been attempted explicitly since neither nuclear burning and diffusion nor turbulent mixing can be properly described by simplified prescriptions (see, however, Lisewski et al.[20]). Phenomenologically, the laminar flame structure is believed to be disrupted by turbulence and to form a distribution of reaction zones with various lengths and thicknesses. In order to find the critical density for the transition between both regimes, we need to formulate a specific criterion for flamelet breakdown. A criterion for the transition between both regimes is discussed in[27,26] and[14]:

$$l_{\rm cutoff} \leq \delta \ . \tag{2}$$

Inserting the results of[41] for $S_{\rm l}$ and δ as functions of density, and using a typical turbulence velocity $v(10^6{\rm cm}) \sim 10^7$ cm s^{-1}, the transition from flamelet to distributed burning can be shown[26] to occur at a density of $\rho_{\rm dis} \approx 10^7$ g cm^{-3}.

4 Modeling turbulent thermonuclear combustion

Next we will outline a way by which several of the ideas discussed in the previous sections can be incorporated into a numerical scheme to model thermonuclear combustion in SN Ia.

Numerical simulations of any kind of turbulent combustion have always been a challenge, mainly because of the large range of length scales involved. In type Ia supernovae, in particular, the length scales of relevant physical processes range from 10^{-3}cm for the Kolmogorov-scale to several 10^7cm for typical convective motions. Despite considerable progress in the field of modeling turbulent combustion for astrophysical flows (see, e.g., Niemeyer & Hillebrandt[24]), the correct numerical representation of the thermonuclear deflagration front is still a weakness of the simulations. Methods used up to now are based on for the reactive-diffusive flame model[11], which artificially stretches the burning region over several grid zones to ensure an isotropic flame propagation speed. However, the soft transition from fuel to ashes stabilizes the front against hydrodynamical instabilities on small length scales, which in turn results in an underestimation of the flame surface area and – consequently – of the total energy generation rate. Moreover, because nuclear fusion rates depend on temperature nearly exponentially, one cannot use the zone-averaged values of the temperature obtained this way to calculate the reaction kinetics.

Therefore we have decided to use a front tracking method to cure some of these weaknesses. The method is based on the so-called *level set technique* which was originally introduced by Osher and Sethian[29]. They used the zero level set of a n-dimensional scalar function to represent $(n-1)$-dimensional front geometries. Equations for the time evolution of such a level set which is passively advected by a flow field are given in Sussman et al.[40]. The method has been extended to allow the tracking of fronts propagating normal to themselves, e.g. deflagrations and detonations[39,36,35]. In contrast to the artificial broadening of the flame in the reaction-diffusion-approach, this algorithm is able to treat the front as an exact hydrodynamical discontinuity. We will demonstrate that such a method can be applied to the supernova problem and, in addition, we will show that even if one attempts to model the physics of thermonuclear burning on unresolved length scales well by physically motivated “Large Eddy Simulations” (LES), one still has to perform calculations with very high spatial resolution in order to verify the correctness of the employed model for the sub-grid scales.

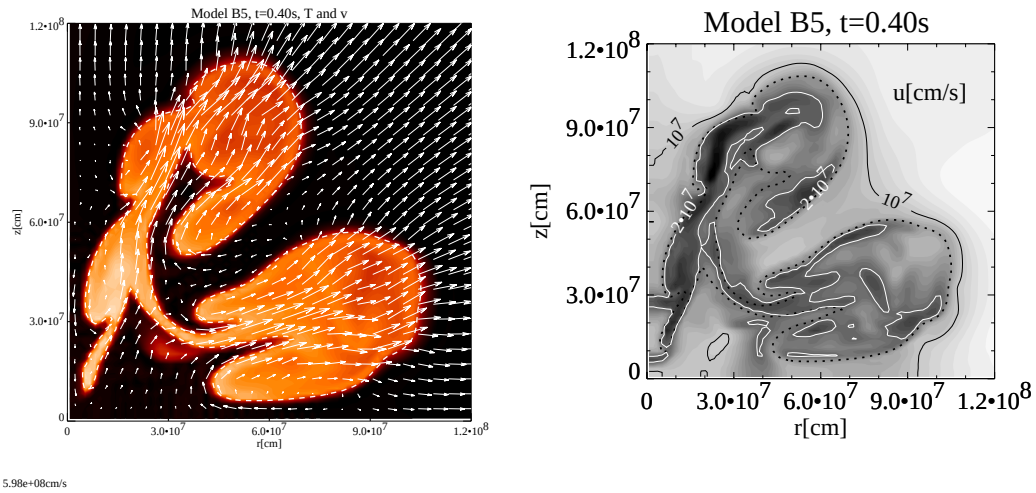

Figure 1: Snapshots of the temperature and the front geometry at 0.4s for model B5 of Reinecke et al. (left figure) and turbulent velocity fluctuations on the grid scale (right panel). The position of of the front is indicated by the dotted curve.

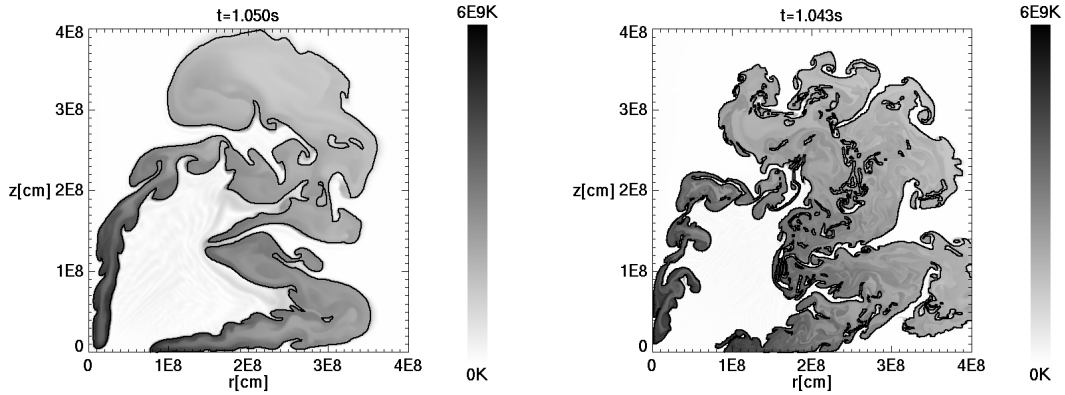

Figure 2: Snapshots of the temperature and the front geometry at 1.05s, taken for the low-resolution model (left figure) and high-resolution run, respectively.

5 Application to the supernova problem

We have carried out two-dimensional numerical simulations in cylindrical rather than in spherical coordinates, mainly because it is much simpler to implement the level set on a Cartesian (r,z) grid. Moreover, the CFL condition is somewhat relaxed in comparison to spherical coordinates. The grid we used in most of our simulations maps the white dwarf onto 256×256 mesh points, equally spaced for the innermost 226×226 zones by Δ=1.5·10^{6}cm, but increasing by 10% from zone to zone in the outer parts. The white dwarf, constructed in hydrostatic equilibrium for a realistic equation of state, has a central density of 2.9·10^{9}g/cm^3, a radius of 1.5·10^{8}cm, and a mass of 2.8·10^{33}g, identical to the one used by Niemeyer and Hillebrandt[24]. The initial mass fractions of C and O are chosen to be equal, and the total binding energy turns out to be 5.4·10^{50}erg. At low densities ($\rho \leq 10^7$g/cm^3), the burning velocity of the front is set equal to zero because the flame enters the distributed regime and our physical model is no longer valid. However, since in reality some matter may still burn the energy release obtained in the simulations is probably somewhat too low.

Here we present only the results for two models, one in which nuclear burning was ignited off-center in a blob and a second one in which initially five blobs were burned as an initial condition, and refer to Reinecke et al.[35] for simulations with other initial conditions.

First, in Fig.1 a snapshot of the "five-blob" model B5 is shown at t = 0.4s. The left panel gives the position of the burning front, the temperatures (in gray-shading), and the expansion velocities. The right panel shows the distribution of turbulent velocity fluctuations. We find that, in accord with one's intuition, most of the turbulence is generated in a very thin layer near the front. Since in the limit of high turbulence intensity the nuclear flames propagate with the turbulent velocity it is obvious that this propagation velocity exceeds the laminar flame speed. However, for most of the initial conditions we have investigated this increase was not sufficient to unbind the star. In fact, model B5 of Reinecke et al. [35] was the only one of the set that did explode.

Moreover, we show the results obtained with 3 times higher resolution for comparison. Fig.2 gives a snapshot taken at 1.05s after ignition for the low-resolution run (left figure) and the high-resolution run, respectively. Although the increase in spatial resolution is only a factor of 3, the right panel shows clearly more structure. This is an important effect because in the flamelet regime the rate of fuel consumption, in first order, increases proportional to surface area of the burning front. The net effect is that the low-resolution model stays bound at the end of the computations, whereas the better resolved model explodes with an explosion energy of about 2×10^{50}erg. Fig.2 also demonstrates that the level-set prescription allows to resolve the structure of the burning front down almost to the grid scale, thus avoiding artificial smearing of the front which is an inherent problem of front-capturing schemes. We want to stress that this gain of accuracy is not obtained at the expense of smaller CFL time steps because in our hybrid scheme the hydrodynamics is still done with cell-averaged quantities.

Unfortunately, the noticeable increase in the total energy release for the better resolved simulation is a strong indication for problems with our sub-grid scale model. Ideally the increased flame surface should have been exactly balanced by a smaller S_t, and the total amount of released energy should not have changed much. This aspect has to be investigated further before convincing predictions about the explosion energetics can be made. Nevertheless the results of the better resolved model are expected to be more accurate since a larger scale range is covered by direct simulation and the sub-grid model should be less important.

Recently wehaveperformed the first three-dimensional supernova simulation based on the presented numerical models. The calculation was carried out on a cartesian grid of 256^3 cells with the same spacing as described for the 2D case. To save computation time, only an octant of the star was simulated and reflecting boundaries were imposed on the coordinate planes, which can be interpreted as an eightfold symmetry. This time the star was ignited in the center, with a perturbation of the radius of the ignited region depending on ϑ. This situation is the three-dimensional equivalent to the model C3 presented in[35]. Figure 3 shows a snapshot of the front geometry after 0.5s. It is evident that the initial axial symmetry has disappeared completely, resulting in a larger flame surface than in the 2D case where the symmetry was artificially enforced. As a consequence, the energy release is considerably higher in three dimensions and is more than sufficient to unbind the star, whereas the corresponding 2D model was only marginally unbound.

We want to stress again, however, that the numerical simulations described here, although leaving behind unbound white dwarfs in several cases, would not fit the observed spectra of SN Ia, mainly because the expansion velocity of the partially burnt gas is too low.

6 Summary and conclusions

In this article we have outlined our present understanding of the explosin mechanism of Type Ia supernovae. From the tremendous amount of work carried out over the last couple of years it has become obvious that the physics of SNe Ia is very complex, ranging from the possibility of very different progenitors to the complexity of the physics leading to the explosion and

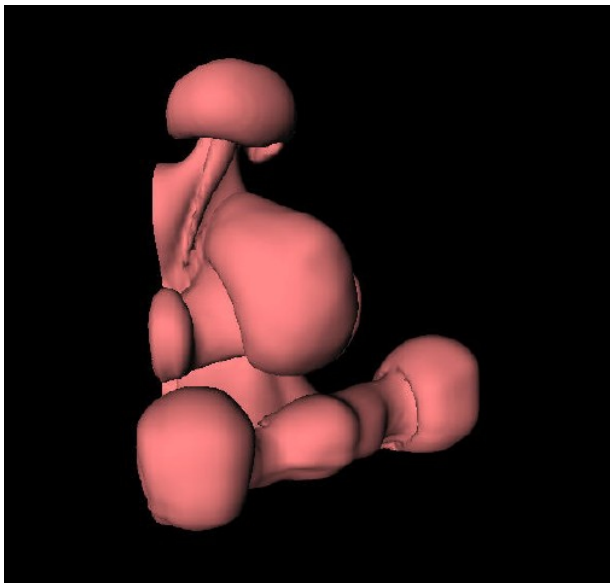

Figure 3: Flame surface in the three-dimensional C3 model at t=0.5s. The integral scale of the flame is about $1.5 \cdot 10^8$cm.

the complicated processes which couple the interior physics to observable quantities. None of these problems is fully understood yet, but what one is tempted to state is that, from a theorist's point of view, it appears to be a miracle that all the complexity seems to average out in a mysterious way to make the class so homogeneous. In contrast, as it stands, a safe prediction from theory seems to be that SNe Ia should get more divers with increasing observed sample sizes. If, however, homogeneity would continue to hold this would certainly add support to the Chandrasekhar-mass scenario discussed in this article. On the other hand, even an increasing diversity would not rule out Chandrasekhar-mass progenitors for most of them. In contrast, there are ways to explain how the diversity is absorbed in a one parameter family of transformations, such as the Phillips relation[32,7] or modifications of it[37,30].

As far as the explosion/combustion physics and the numerical simulations are concerned significant recent progress has made the models more realistic (and reliable). Thanks to ever increasing computer resources 3-dimensional simulations have become feasible which treat the full star with good spatial resolution and realistic input physics. Already the results of 2-dimensional simulations indicate that pure deflagrations waves in Chandrasekhar-mass C+O white dwarfs can lead to explosions, and going to three dimensions, because of the increasing surface area of the nuclear flames, further adds to the explosion energy. On the side of the combustion physics, the burning in the distributed regime at low densities needs to be explored further, but it is not clear anymore whether a transition from a deflagration to a detonation in that regime is needed for successful models. In fact, according to recent studies such a transition appears to be rather unlikely.

Acknowledgments

This work was supported in part by the Deutsche Forschungsgemeinschaft under Grant Hi 534/3-1, the DAAD, and by DOE under contract No. B341495 at the University of Chicago. The computations were performed at the Rechenzentrum Garching on a Cray J90.

1. Arnett, W. D., and Livne, E., *ApJ*, 427:31, 1994.
2. Buchler, J. R.,, Colgate, S. A., and Mazurek, T. J., *Journal de Physique*, 41:2, 1980.

3. Clavin, P., *Annual Rev. Fluid Mech.*, 26:321, 1994.
4. Courant, R., and Friedrichs, K. O., *Supersonic Flow and Shock Waves*. Springer, New York, 1948.
5. Damköhler, G., *Z. Elektrochem.*, 46:601, 1940.
6. Fermi, E., In E. Segre, editor, *Collected Works of Enrico Fermi*, pages 816–821. 1951.
7. Hamuy M., Phillips M. M., Suntzeff N. B., Schommer R. A., et al., *AJ* 109:1, 1996.
8. Ivanova, L. N., Imshennik, V. S., and Chechetkin, V. M., *Pis ma Astronomicheskii Zhurnal*, 8:17, 1982.
9. Khokhlov, A. M., *A&A*, 245:114, 1991.
10. Khokhlov, A. M., *A&A*, 245:L25, May 1991.
11. Khokhlov, A. M., *ApJL*, 419:L77, 1993.
12. Khokhlov, A. M., *ApJL*, 424:L115, 1994.
13. Khokhlov, A. M., *ApJ*, 449:695, 1995.
14. Khokhlov, A. M., Oran, E. S., and Wheeler, J. C., *ApJ*, 478:678, 1997.
15. Kolmogorov, A. N., *Dokl. Akad. Nauk SSSR*, 30:299, 1941.
16. Landau, L. D., and Lifshitz, E. M., *Fluid Mechanics*. Butterworth-Heinemann, xxx, 1995.
17. Layzer, D., *ApJ*, 122:1, 1955.
18. Lewis, B., and von Elbe, G., *Combustion, Flames, and Explosions of Gases*. Academic Press, New York, 2nd edition, 1961.
19. Livne, E., *ApJL*, 406:L17, 1993.
20. Lisewski, A. M., Hillebrandt, W., Woosley, S. E., Niemeyer, J. C., and Kerstin, A. R., *ApJ*, in print, 2000.
21. Müller, E., and Arnett, W. D., *ApJL*, 261:L109, 1982.
22. Müller, E., and Arnett, W. D., *ApJ*, 307:619, 1986.
23. *ApJL*, 523:L57, 1999.
24. Niemeyer, J. C., and Hillebrandt, W., *ApJ*, 452:769, 1995.
25. Niemeyer, J. C., and Hillebrandt, W., Microscopic and macroscopic modeling of thermonuclear burning fronts. In P. Ruiz-Lapuente, R. Canal, and J. Isern, editors, *Thermonuclear Supernovae*, pages 441–456, Dordrecht, 1997. Kluwer.
26. Niemeyer, J. C., and Kerstein, A. R., Burning regimes of nuclear flames in sn ia explosions. *New Astronomy*, 2:239, 1997.
27. Niemeyer, J. C., and Woosley, S. E., *ApJ*, 475:740, 1997.
28. Nomoto, K., Thielemann, F. K., and Yokoi, K., *ApJ*, 286:644, 1984.
29. Osher, S., and Sethian, J. A., *JCP*, 79:12, 1988.
30. Perlmutter S., Gabi S., Goldhaber G., Goobar A, Groom D. E., et al., *ApJL* 483:565, 1997.
31. Peters, N., In *Symp. (Int.) Combust., 21st*, pages 1232, Pittsburgh, 1988. Combustion Institute.
32. Phillips M. M., *ApJL*, 413:L105, 1993.
33. Pope, S. B., *Annual Rev. Fluid Mech.*, 19:237, 1990.
34. Read, K. I., *Physica D*, 12:45, 1984.
35. Reinecke, M., Hillebrandt, W., and Niemeyer, J. C., *A&A*, 347:739, 1999.
36. Reinecke, M., Hillebrandt, W., Niemeyer, J. C., Klein, R., and Gröbl, A., *A&A*, 347:724, 1999.
37. Riess A. G., Press W. H., Kirshner R. P., *ApJ* 473:88, 1996.
38. Sharp, D. H., *Physica D*, 12:3, 1984.
39. Smiljanovski, V., Moser, V., and Klein, R., *Combust. Theory Modelling*, 1:183, 1997.
40. Sussman, M., Smereka, P., and Osher, S., *JCP*, 114:146, 1994.
41. Timmes, F. X., and Woosley, S. E., *ApJ*, 396:649, 1992.
42. Williams, F. A., *Combustion Theory*. Benjamin / Cummings, Menlo Park, 2nd edition, 1985.

43. Woosley, S. E., and Weaver, T. A., The physics of supernovae. In Dimitri Mihalas and Karl-Heinz A. Winkler, editors, *Radiation Hydrodynamics in Stars and Compact Objects, Lecture Notes in Physics*, volume 255, pages 91, Berlin, 1986. Springer.
44. Woosley, S. E., Type Ia supernovae: Carbon deflagration and detonation. In A. G. Petschek, editor, *Supernovae*, pages 182, Berlin, 1990. Springer.
45. Youngs, D. L., *Physica D*, 12:32, 1984.
46. Zeldovich, Y. B., Barenblatt, G. I., Librovich, V. B., and Makhviladze, G. M., *The Mathematical Theory of Combustion and Explosions*. Plenum, New York, 1985.